ACS Catalysis

RESEARCH ARTICLE

pubs.acs.org/acscatalysis

Synthesis, Characterization, and Heterogeneous Catalytic Implementation of Sulfated Alumina Nanoparticles. Arene Hydrogenation and Olefin Polymerization Properties of Supported Organozirconium Complexes

Linda A. Williams and Tobin J. Marks*

Department of Chemistry, Northwestern University, Evanston, Illinois 60208-3113, United States

ABSTRACT: Sulfated alumina nanoparticles (n-AlS) have been prepared as a high-surface-area support/activator for organozirconium catalysts. The large external surface area allows chemisorption of ca. 3 times more organozirconium catalyst per square nanometer than previously possible on bulk sulfated alumina. It is found that Cp^*ZrMe_2/n-AlS ($Cp^* = \eta^5$-$(CH_3)_5C_5$, Me = CH_3) and $ZrBz_3$/n-AlS (Bz = $CH_2C_6H_5$) are active catalysts for arene hydrogenation as well as for olefin polymerizations. The less sterically encumbered $ZrBz_3$/n-AlS exhibits higher polymerization activity and a greater arene hydrogenation turnover frequency than the slightly more encumbered Cp^*ZrMe_2/n-AlS. Catalyst $ZrBz_3$/n-AlS also displays a larger tolerance for sterically demanding hydrogenation substrates as well as increased 1-hexene incorporation in ethylene/1-hexene copolymerizations.

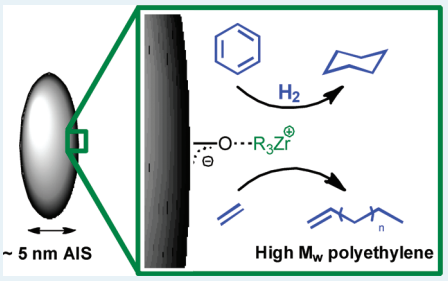

KEYWORDS: sulfated alumina nanoparticles, arene hydrogenation, olefin polymerization, zirconocene

INTRODUCTION

At the interface between traditional homo- and heterogeneous catalysts, single-site supported catalysts have generated much academic and industrial research interest in recent years.[1−6] In parallel, there has also been intense recent interest in using nanometer-sized particles as catalyst supports.[7−12] Such nanoparticle supports may offer advantages over bulk supports, such as increased surface area, better heat and mass transfer, and decreased internal surface area.[13−16] The latter point is particularly important in the case of olefin polymerization, where steric crowding around the metal center and the growing polymer chain may lead to decreased activities, adverse mass transport effects, or both.[17,18] Heterogenizing molecular catalysts also allows the use of slurry reactors,[19−22] which are advantageous owing to their excellent heat transfer, amenability to efficient online catalyst addition or withdrawal, and ease of construction.[23] Chemisorption of discrete organometallic complexes on metal oxide supports has been shown to yield catalysts, which have reasonably well-defined active sites, greater catalyst stability, and lend to decreased reactor fouling versus the analogous homogeneous systems.[24,25] These supported catalysts have been shown to exhibit very high activity for α-olefin polymerizations[26−35] as well as for catalytic hydrocarbon transformations.[36−44]

Previously, this laboratory investigated the chemisorption pathways of ^{13}C-enriched organogroup 4[45−49] and organoactinide[50−57] metal hydrocarbyls on various metal oxides surfaces. It was demonstrated that the acidity and related surface chemical properties of the support determine which of three distinctive chemisorption pathways is operative. Heterolytic M−C bond scission, in which an alkide group is transferred to a surface Lewis acid site and affords a "cationic" adsorbate species, (e.g., structure **A**) is the primary chemisorptive pathway for Lewis acidic surfaces, including $MgCl_2$, as well as for highly and partially dehydroxylated alumina (Figure 1).[50−57] This reaction finds strong chemical analogy (and chemical/spectroscopic similarity) to analogous heterolysis processes effected in solution by organo-Lewis acids such as perfluoroaryl boranes and MAO (e.g., eq 1).[58−66] For weakly Brønsted acidic surfaces, such as partially dehydroxylated silica and MgO, M−CH_3 protonolysis yields catalytically less active "μ-oxo" species (e.g., structure **B**). This process also has close homogeneous phase analogies (e.g., eq 2).[67] The depressed activity of species **B** versus **A** can be attributed to the formation of the strong oxo conjugate base of the weak surface Bronsted acid site, which coordinates strongly to the hard Lewis acidic metal center, saturating the coordination sphere and depressing the electrophilicity.

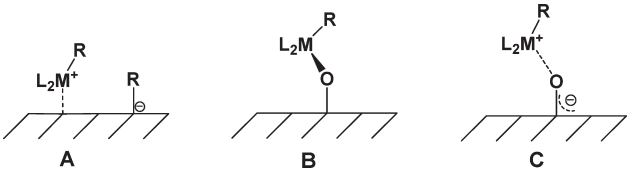

$$Cp_2ZrMe_2 + B(C_6F_5)_3 \rightarrow Cp_2ZrMe^+MeB(C_6F_5)_3^- \quad (1)$$

Received: December 6, 2010
Revised: February 3, 2011
Published: February 21, 2011

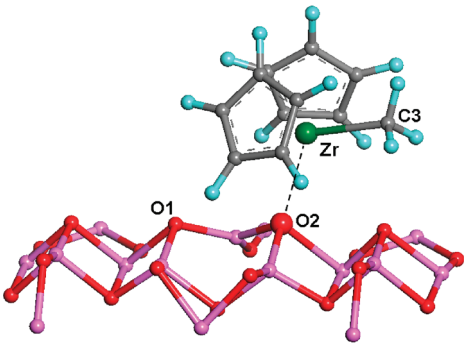

Figure 1. Computed energy-minimized structure of Cp_2ZrMe^+ cation coordination to a μ_3-O alumina surface site.[46]

$$Cp_2ZrMe_2 + HOAr \rightarrow Cp_2ZrMe(OAr) + CH_4 \quad (2)$$

$$Cp^*_2ZrMe_2 + R_3NH^+BPh_4^- \rightarrow Cp^*_2ZrMe^+BPh_4^- + MeH + NR_3 \quad (3)$$

Recent studies of metal hydrocarbyl chemisorption on highly Brønsted acidic sulfated metal oxides, including sulfated zirconia[68−74] and sulfated alumina,[75,76] indicate that M−C σ-bond protonolysis occurs readily at the strong Brønsted acidic sites. This reactivity is analogous to the solution protonolysis effected by ammonium aryl borates (e.g., eq 3).[77] The product of this chemisorptive process is a highly reactive "cation-like" surface organometallic electrophile (e.g., structure **C**) with nearly 100% of the surface sites displaying catalytic activity for ethylene polymerization and arene hydrogenation.[47] Theoretical studies have shown that the organometallic cation−oxo anion interaction in **C** is nondirectional and largely electrostatic in nature (Figure 2).[47,78] One of the great attractions of sulfated metal oxides as catalyst supports is the low cost and ease of preparation, while at the same time they provide sufficient acidity to simultaneously activate and immobilize the catalyst. This immobilization-based activation eliminates the use of expensive cocatalysts, such as MAO, or noncoordinating anions, such as $B(C_6F_5)_4^-$, while simultaneously suppressing complications such as catalyst leaching associated with these organic cocatalysts in heterogeneous systems.

Sulfated metal oxides are so-called solid "super acids", meaning that their Brønsted acidity is greater than that of sulfuric acid.[79] A variety of bulk solid super acids have been studied, including sulfated Al_2O_3,[80−87] Fe_2O_3,[88] HfO_2,[89] SiO_2,[90] SnO_2,[91−93] TiO_2,[94,95] and ZrO_2,[96] and the sulfate modification of these metal oxides has been shown to greatly enhance hydrocarbon skeletal rearrangement rates. Alumina is of great importance as a high-surface-area support in industrial catalysis, and therefore, increased understanding and implementation of sulfated alumina as a catalyst support is particularly relevant. There has been limited research into the catalytic properties of nanosized sulfated metal oxides,[97] and little is known about the properties of nanosized sulfated alumina. Lima, et al. reported efforts to control the acidity of nanocapsular sulfated alumina synthesized by the sol−gel method; however, they achieved limited control over the morphology of the alumina.[98]

In this contribution, we report the facile surface modification of preformed γ-alumina nanoparticles with sulfuric acid as a preferred synthetic route to nanosized sulfated alumina. We describe here the synthesis, microstructural characterization, and heterogeneous catalytic implementation of these sulfated alumina nanoparticles. It will be seen that sulfated alumina nanoparticles offer a high-surface-area catalyst support/activator for organozirconium catalysts and that the supported catalysts are active for olefin polymerization and arene hydrogenation.

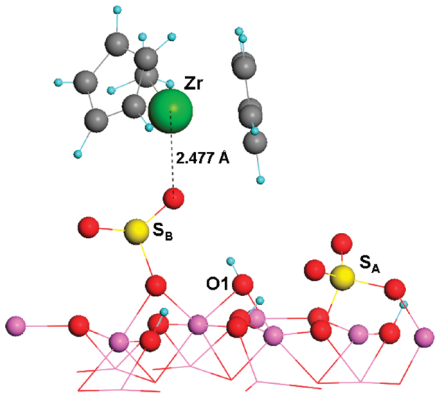

Figure 2. Computed energy-minimized structure of Cp_2ZrMe^+ cation coordination to an S═O fragment of an AlS surface sulfate group, showing the electrostatic interaction between the deprotonated surface Brønsted acid site and the cationic zirconium metal center.[78]

EXPERIMENTAL SECTION

All procedures for air- and moisture-sensitive compounds were carried out with rigorous exclusion of O_2 and moisture in flame- or oven-dried Schlenk-type glassware interfaced to a dual manifold Schlenk line or a high-vacuum ($10^{-5} - 10^{-6}$ Torr) line or in a nitrogen-filled M-Braun glovebox with a high capacity recirculator (<1 ppm O_2). Argon (Airgas, prepurified) was purified by passage through MnO/vermiculite and Davidson 4A molecular sieve columns. Oxygen (Airgas) was purified by passage through Drierite (Hammond Co.). All hydrocarbon solvents (*n*-pentane, toluene, benzene) were distilled from Na/K alloy. All organic starting materials were purchased from Aldrich Chemical Co, and used without further purification unless otherwise noted. Deuterated benzene was purchased from Cambridge Isotope Laboratories (>99 atom % D), dried over Na/K alloy, and stored in resealable flasks. The substrate *m*-xylene (Aldrich) was dried over CaH_2 and vacuum-transferred into a storage tube containing activated 4A molecular sieves. The organometallic complex Cp^*ZrMe_3 was synthesized by the literature procedure.[99] The ^{13}C-labeled complex $Cp^*_2Zr^{13}Me_2$[100] was synthesized from $^{13}CH_3Li\cdot LiI$ prepared from $^{13}CH_3I$[101] (99% ^{13}C, Cambridge Isotope Laboratories) using analogous methods. The organometallic complex $ZrBz_4$ was purchased from Strem and used without modification.

Physical and Analytical Measurements. Solution NMR spectra were recorded on either a Varian Inova-400 (FT, 400 MHz, ^{1}H; 100 MHz, ^{13}C) or an Inova-500 (FT, 500 MHz, ^{1}H; 125 MHz, ^{13}C) spectrometer. ^{1}H and ^{13}C NMR experiments on air-sensitive solution samples were conducted in Teflon valve sealed sample tubes (J-Young). ^{13}C CPMAS solid-state NMR spectra were recorded on a Varian VXR400 (FT, 100 MHz, ^{13}C). For ^{13}C CPMAS solid-state NMR spectroscopy, air-sensitive samples were loaded into cylindrical zirconia rotors in the glovebox and capped with a solid Teflon cap. For routine spectra of organozirconium adsorbates, the cross-polarization contact time was 2 ms, and the recycle time was 5 s. For adsorbed

dx.doi.org/10.1021/cs100119w |*ACS Catal.* 2011, 1, 238–245

complexes, 16 000 scans were required to obtain satisfactory signal:noise ratios, with a spinning rate of 10 kHz, depending on peak location versus the location of spinning sidebands. BET surface area measurements were performed on a Micromeritics ASAP 2010 instrument. Inductively coupled plasma (ICP) spectroscopy was conducted on a Varian model ICP spectrometer equipped to cover the spectral range from 175 to 785 nm. An aliquot of concentrated acid solution was diluted to 5% with DI H_2O and analyzed for S (181.972 nm) and Zr (343.823 nm) content as compared with standardized solutions. GC data were collected on an HP6890 GC/MS equipped with an HP5972 detector and an HP-5MS (5% phenyl methyl siloxane, 30 m × 250 μm × 0.25 μm) capillary column. TEM imaging was performed on a Hitachi HF-2000 analytical electron microscope. Powder XRD data were recorded on a Rigaku DMAX-A diffractometer with Ni-filtered Cu Kα radiation (1.541 84 A°).

Synthesis of Nano-Sized Sulfated Alumina. Nanosized sulfated alumina was synthesized by a modification of the literature procedure.[47] γ-Alumina nanoparticles (25 nm, Nanostructed and Amorphous Materials Inc.) were calcined at 550 °C for 3 h in 100 mL/min flowing O_2. To 15 g of this material was added 150 mL of 3.2 M H_2SO_4, and the resulting slurry was stirred for 1 h. The slurry was then centrifuged (8000 rpm, 10 min), the supernatant was decanted, and the solid was washed with deionized water until the supernatant was no longer acidic. Next, the sample was dried overnight at 120 °C, crushed to <80 mesh, then calcined at 550 °C for 3 h in flowing O_2 (100 mL/min). Finally, the sulfated alumina was activated under high vacuum (5×10^{-6} Torr) at 450 °C for 45 min and stored under a dry N_2 atmosphere. The BET surface area was 237 m^2/g, consisting exclusively of external surface area. ICP analysis of the sample digested overnight in HF indicated that the sulfur loading was 2.81 atoms S/nm^2.

Chemisorption of Organozirconium Complexes on Nano-Sized Sulfated Alumina. In a two-sided flip-fritted reaction vessel, 25 mL pentane was condensed onto carefully weighed quantities of organometallic precursor and nanosized sulfated alumina support. The slurry was then stirred at 25 °C for 1 h and filtered. The supported catalyst was collected on the frit, washed five times with pentane to remove any physisorbed catalyst, then dried in vacuo for 1 h. The prepared catalysts were stored in sealed containers under a dry N_2 atmosphere at −40 °C until used. If greater than saturation coverage of the organozirconium complexes was used, excess unreacted organozirconium complex could be detected in the opposite flask after washing. The supported catalyst was checked by slurry-phase NMR spectroscopy in C_6D_6 to ensure that no physisorbed catalyst remained on the support after the pentane washing. When a sample synthesized in this manner was analyzed by ICP spectroscopy following digestion overnight with 48% HF, the maximum loadings of organozirconium complexes and sulfur present were 0.87 atom of Zr/nm^2 (3.42×10^{-7} mol Zr/mg n-AlS) and 2.94 atoms of S/nm^2.

Arene Hydrogenations. In a typical experiment, a 15 mL water-jacketed Morton flask, dried overnight in a 160 °C oven, was charged in the glovebox with 60−100 mg of supported catalyst and 2.0 mL of dry substrate. The closed reactor was then removed from the glovebox, interfaced to the high vacuum line, and freeze−pump−thaw-degassed at −78 °C. The reactor was then connected to a constant temperature circulating pump and equilibrated for 15 min at 31.0 °C. The flask was agitated using a vortex mixer (2000 rev/min), and hydrogen was added to the flask and maintained at 1.0 atm with a Hg bubbler. To determine the catalytic turnover frequency, aliquots of the reaction solution (5 μL) were removed at designated times, and conversion was monitored by GC/MS.

Ethylene Homopolymerizations. In a typical experiment, a 300 mL, medium-pressure, glass reaction vessel dried overnight in a 160 °C oven was charged in the glovebox with 30−60 mg of supported catalyst, a magnetic stirbar, and 10 mL of dry toluene. The closed reactor was removed from the glovebox, interfaced to the high-pressure line behind a blast shield, and freeze−pump−thaw-degassed at −78 °C. The reactor was then warmed to the desired temperature using an external bath and equilibrated for 5 min, charged with 75 psi ethylene pressure, and stirred rapidly (>1500 rpm) to minimize mass transport effects. After 10−60 min, the pressure was released, and the polymerization was quenched with methanol. The polymeric product was collected by filtration, dried overnight in vacuo at 60 °C, and weighed.

Ethylene +1-Hexene Copolymerizations. In a typical experiment, a 300 mL, medium-pressure reaction vessel, dried overnight in a 160 °C oven, was charged in the glovebox with 30−60 mg supported catalyst, a magnetic stirbar, and 10 mL of dry toluene. The closed reactor was removed from the glovebox, interfaced to the high-pressure line behind a blast shield, freeze−pump−thaw-degassed at −78 °C, and warmed to the desired temperature with an external bath. Ethylene was added to the reactor and maintained at 1.0 atm, while 2.0 mL of 1-hexene comonomer was immediately added to the reactor by gastight syringe, with rapid stirring. The reactor was then pressurized to 75 psi ethylene and stirred rapidly (>1500 rpm) to minimize mass transport effects. After 30−60 min, the pressure was released, and the polymerization was quenched with methanol. The polymeric product was collected by filtration, dried overnight in vacuo at 60 °C, and weighed.

RESULTS AND DISCUSSION

This section begins with discussion of the synthesis and characterization of nanosized sulfated alumina (n-AlS) supports, including SS-NMR spectroscopy of the supported catalysts. Next, arene hydrogenations mediated by Cp^*ZrMe_2/n-AlS and $ZrBz_3$/n-AlS will be discussed. Finally, the ethylene homopolymerization as well as ethylene/1-hexene copolymerization properties of Cp^*ZrMe_2/n-AlS and $ZrBz_3$/n-AlS are investigated.

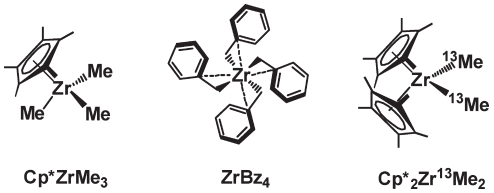

Cp^*ZrMe_3 $ZrBz_4$ $Cp^*_2Zr^{13}Me_2$

Support Preparation and Characterization. There are several preparative methods for sulfated alumina that have been reported in the literature.[47,102,103] For the present study, the surface modification of commercially available 25 nm γ-alumina nanoparticles with sulfuric acid was used as the preferred method of sulfated alumina preparation. In contrast to bulk γ-alumina, nanosized γ-alumina requires a presulfonation calcination at 550 °C to remove residual surfactants present from the

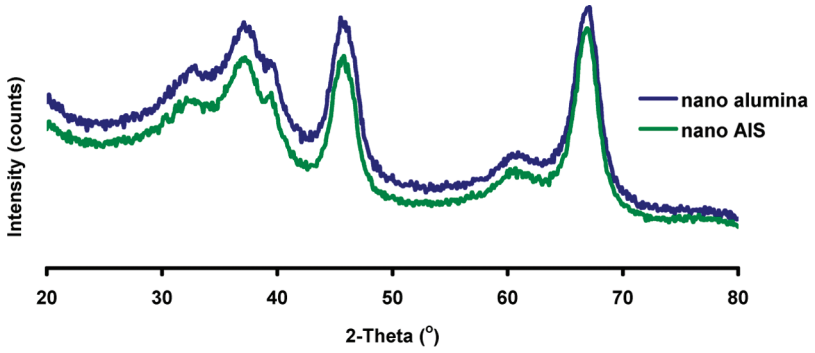

Figure 3. X-ray diffraction pattern of nanocrystalline γ-Al_2O_3 (a) and nanocrystalline γ-sulfated alumina (b). Intensity is in arbitrary units.

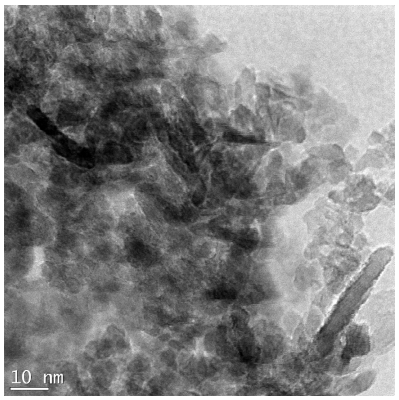

Figure 4. TEM image of nano AlS.

nanoparticle synthesis. For the present n-AlS, the BET surface area was 237 m^2/g, with almost exclusively external surface area. XRD analysis of the alumina nanoparticles before and after sulfonation reveals that the alumina is predominantly present as the γ phase, and there is no change in phase resulting from the harsh sulfonation/calcination conditions (Figure 3). Fitting of the diffraction peak widths at half-maximum to the Debye−Scherrer equation reveals the n-AlS to have average crystallite sizes of ∼4 nm. TEM analysis of the nanoparticles indicates that the nanoparticles are loosely aggregated nanorods with radii of ∼5 nm and lengths of ∼10−30 nm (Figure 4).

Catalyst Synthesis. All organozirconium catalyst precursors used in this study were synthesized as described elsewhere.[97,98] To determine the effects of ancillary ligation and sterics on catalytic activity, mono(pentamethylcyclopentadienyl) and homoleptic hydrocarbyl zirconium complexes were employed as adsorbates on the present sulfated alumina nanoparticles (n-AlS). Bulk AlS as prepared previously has been reported to be "super acidic" with the ability to simultaneously support and activate organozirconium complexes.[45,47] Chemisorption of the precursors was carried out under rigorously anhydrous/anaerobic conditions, and the supported catalysts were washed repeatedly with pentane to remove any physisorbed/weakly bound neutral species.

Structural Characterization of Adsorbate Species. Chemisorption of organozirconium complexes onto n-AlS was studied by solid-state ^{13}C CPMAS NMR spectroscopy using the ^{13}C-labeled probe complex $Cp^*_2Zr^{13}Me_2$ and monitoring the fate of the ^{13}C-labeled methyl groups originally coordinated to Zr. $Cp^*_2Zr^{13}Me_2$ was used as a model complex owing to its good thermal stability over the time frame necessary for the NMR experiment (24 h) as well as to compare the chemisorption reaction of $Cp^*_2Zr^{13}Me_2$ on n-AlS to that on bulk AlS and the homogeneous metallocenium species reported in the literature. As can be seen in Figure 5, the ^{13}C CPMAS NMR spectrum of $Cp^*_2Zr^{13}Me$/n-AlS exhibits major resonances at δ 123.3, 43.0, 9.0, and −9.8. Data and assignments are summarized in Table 1. The resonances at δ 123.3 and 9.0 are readily assigned to Cp ring carbon atoms and Cp-CH_3 carbon atoms, respectively, and are analogous to the solution phase NMR data (Table 1.) The minor resonance at δ −9.8 can be attributed to a ^{13}C-labeled methyl group that is transferred to a Lewis acid site on the surface forming an Al−$^{13}CH_3$ moiety (structure **A**).[47] The intense resonance at δ = 43.0 is assignable to a "cation-like", electron-deficient $Cp^*_2Zr^{13}Me^+$ species (structure **C**), as evidenced by the marked downfield shift of the resonance from the neutral molecule (δ 36.8), and finds analogy in the δ (Zr−CH_3) downfield shift of the well-characterized homogeneous analogue $Cp^*_2Zr^{13}Me^+Q^-$ at δ = 50.4 for Q^- = $CH_3B(C_6F_5)_3^-$.[104] The present chemisorption pathways for organozirconium complexes supported on n-AlS are then very similar to previous results on bulk AlS,[47] with the only difference observed being the small amount of methide transfer to the Lewis acidic sites (δ = −9.8) seen in the n-AlS sample (structure **A**, above). Formation of the μ-oxo species (structure **B**, δ ∼ 32 ppm) is not evident.[47] ICP characterization of the supported catalysts indicates that surface coverage of the organozirconium is 0.87 Zr atom/nm^2 for $ZrBz_3$/n-AlS, and 0.77 Zr atom/nm^2 for Cp^*ZrMe_2/n-AlS. For the same catalysts supported on bulk AlS, 0.25 Zr atom/nm^2 is the highest coverage obtainable.[47] Thus, the nanosized alumina has greater than 3 times more catalyst supported per nanometer. This increase can be attributed to the minimization of internal surface area on the alumina nanoparticles, therefore increasing surface area available to the catalyst (eq 4).

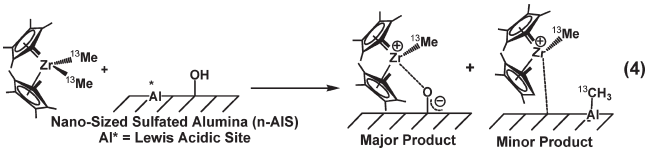

Arene Hydrogenation Experiments. Arene hydrogenation experiments employing Cp^*ZrMe_2/n-AlS and $ZrBz_3$/n-AlS were carried out in the reactor described in the Experimental Section.

dx.doi.org/10.1021/cs100119w |ACS Catal. 2011, 1, 238–245

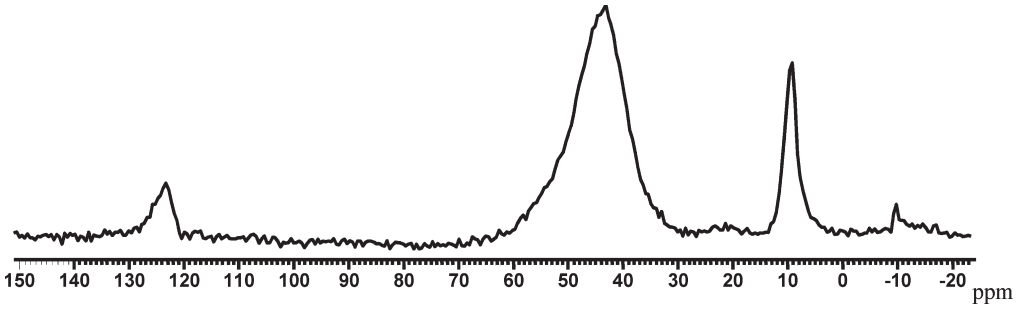

Figure 5. ^{13}C CPMAS NMR spectrum (100 MHz) of Cp*$_2$Zr^{13}Me/n-AlS (16 000 scans, repetition time = 5 s, contact time = 2 ms, spinning speed = 10 kHz).

Table 1. Solid-State ^{13}C NMR Chemical Shift Data in Parts per Million for Neat and Supported Organometallic Complexes[a]

complex	Cp′ ring	M−^{13}C$_\alpha$	Cp′−CH$_3$	Al−CH$_3$
Cp*$_2$Zr^{13}Me$_2$[b,c]	117.4	36.8	12.1	
Cp*$_2$Zr^{13}Me/AlS[c,d]	123.0	46.0	9.1	
Cp*$_2$Zr^{13}Me/n-AlS[e]	123.3	43.0	9.0	−9.8

[a] In parts per million downfield from Me$_4$Si; referenced to the solid-state ^{13}C spectrum of adamantane. [b] Measured in C$_6$D$_6$ solution, Cp* = η^5-(CH$_3$)$_5$C$_5$. [c] Ref 47. [d] AlS = sulfated alumina. [e] n-AlS = nanosized sulfated alumina

Table 2. Arene Hydrogenation Catalyzed by Organozirconium Complexes Supported on Nano-Sized Sulfated Alumina at 31.0 °C, P_{H_2} = 1 atm

entry	catalyst	substrate	N_t[a] h^{-1}
1	Cp*ZrMe$_2$/n-AlS	benzene	15
2	Cp*ZrMe$_2$/n-AlS	toluene	3
3	Cp*ZrMe$_2$/n-AlS	*m*-xylene	∼0
4	ZrBz$_3$/n-AlS	benzene	36
5	ZrBz$_3$/n-AlS	toluene	16
6	ZrBz$_3$/n-AlS	*m*-xylene	3

[a] N_t values determined by GC/MS

Results are summarized in Table 2. These catalysts were chosen because of their steric openness as well as on the basis of previous research, which showed that similar catalysts supported on bulk sulfated alumina are active for arene hydrogenation.[47] Note that these cationic catalysts are electrostatically bound to the support so that catalyst leaching is extremely improbable in hydrocarbon solvents. Neither has it been reported previously for these types of catalysts.[17,18,45,47] Moreover, the neutral precursors are not active for the present hydrogenation processes. In this study, the benzene turnover frequency for ZrBz$_3$/n-AlS at 31 °C, 1 atm H$_2$, was 36 h^{-1} (Table 2, entry 1). Arene hydrogenations mediated by these supported catalysts display complete hydrogenation of benzene to cyclohexane, toluene to methylcyclohexane, etc., with no GC/MS evidence of partially hydrogenated products, such as cyclohexene, etc. For all substrates studied, ZrBz$_3$/n-AlS is found to be significantly more active than Cp*ZrMe$_2$/n-AlS. We propose that the decreased coordinative saturation of ZrBz$_3$/n-AlS versus Cp*ZrMe$_2$/n-AlS is responsible for the increased activities for ZrBz$_3$/n-AlS as well as the ability of ZrBz$_3$/n-AlS to hydrogenate more sterically demanding substrates, such as *m*-xylene. As the steric requirements of the substrate increase, there is a decrease in catalyst turnover frequency and, in the case of *m*-xylene, negligible hydrogenation observed with Cp*ZrMe$_2$/n-AlS.

Olefin Polymerization Experiments. Ethylene homopolymerization studies employing the present organozirconium catalysts on nanosized sulfated alumina were carried out at 150 psi ethylene and 25 °C in a medium-pressure batch reactor with rapid stirring to minimize mass transport effects. Results are summarized in Table 3. It is found that for these supported catalysts, polymerization activities follow the order ZrBz$_3$/n-AlS > Cp*ZrMe$_2$/n-AlS, which tracks the approximate coordinative saturation of the catalysts and repeats the trend seen in the above arene hydrogenation experiments. Polymerizations run with less-coordinating heptane as the reaction solvent were 3−10 times more active than identical polymerizations run in toluene. It is important to note that although solvent choice significantly affects the activity of the supported catalysts, the melting point characterization of the polymeric products by DSC shows that the T_m does not change significantly with a change in reaction solvent and that all products are high-molecular-weight crystalline polyethylene. Attempts to separate the polymer from the supported catalyst were unsuccessful, even at 140 °C in 1,2,4-trichlorobenzene. The formation of such high-molecular-weight polyethylene has also been reported for ethylene polymerizations mediated by related catalyst systems, such as organozirconium adsorbates on alumina,[105] on sulfated zirconia,[48] and on sulfated alumina.[47]

Ethylene/1-hexene copolymerization studies employing Cp*ZrMe$_2$/n-AlS and ZrBz$_3$/n-AlS were performed under reaction conditions identical to those of the ethylene homopolymerizations discussed above with the addition of 1-hexene comonomer (1.6 M). The results of these polymerizations can be seen in Table 4, and activities follow the trend ZrBz$_3$/n-AlS > Cp*ZrMe$_2$/n-AlS at 25 °C. Again, the activity of these catalysts is substantially increased on switching from toluene to heptane as the reaction solvent. DSC melting point characterization of the polymeric products shows that for the polymers produced by Cp*ZrMe$_2$/n-AlS, T_m does not significantly decrease from the homopolymer, indicating limited 1-hexene incorporation,[106] whereas for ZrBz$_3$/n-AlS, the T_m's decrease from 134 to 128 °C, indicating greater 1-hexene incorporation. The less coordinatively saturated the catalyst precursor is (ZrBz$_3$/n-AlS < Cp*ZrMe$_2$/n-AlS), the more active it is for ethylene/1-hexene copolymerization, as well as for enhanced comonomer incorporation selectivity.

dx.doi.org/10.1021/cs100119w |*ACS Catal.* 2011, 1, 238–245

Table 3. Summary of Ethylene Homopolymerization Data for Organozirconium Complexes Supported on Nano-Sized Sulfated Alumina

entry[a]	catalyst[b]	[Zr] (μmol)	reaction solvent	reaction time (min)	PE yield (g)	activity[c] (x10^4)	T_m (°C)
1	Cp*ZrMe$_2$/n-AlS	13.8	toluene	60	0.42	0.6	135
2	Cp*ZrMe$_2$/n-AlS	17.7	heptane	60	0.75	5.6	135
3	ZrBz$_3$/n-AlS	10.3	toluene	30	1.64	6.4	134
4	ZrBz$_3$/n-AlS	12.0	heptane	10	1.93	19.3	133

[a] Carried out at 75 psi ethylene, 10.0 mL of solvent, 25 °C. [b] n-AlS = nanosized sulfated alumina. [c] Units: grams of polymer/(mol Zr × h × atm).

Table 4. Summary of Ethylene/1-Hexene Copolymerization Data for Organozirconium Complexes Supported on Nano-Sized Sulfated Alumina

entry[a]	catalyst[b]	[Zr] (μmol)	[1-hexene] (M)	reaction solvent	reaction time (min)	PE yield (g)	activity[c] (x10^4)	T_m (°C)
1	Cp*ZrMe$_2$/n-AlS	16.0	1.6	toluene	60	0.45	0.6	133
2	Cp*ZrMe$_2$/n-AlS	18.0	1.6	heptane	60	0.73	0.8	134
3	ZrBz$_3$/n-AlS	13.5	1.6	toluene	30	2.38	7.0	129
4	ZrBz$_3$/n-AlS	10.6	1.6	heptane	20	2.16	19.3	128

[a] Carried out at 75 psi ethylene, 10.0 mL of solvent. [b] n-AlS = nanosized sulfated alumina. [c] Units: grams of polymer/(mol Zr × h × atm).

CONCLUSIONS

This contribution provides a straightforward synthesis of sulfated alumina nanoparticles as a support for organozirconium-based heterogeneous arene hydrogenation and olefin polymerization catalysts. The nanosized AlS has a much greater surface area than bulk aluminas previously investigated, as well as minimal internal surface area, which should limit mass transport effects associated with catalysts chemisorbed in pores. The minimization of internal surface area also accounts for the 3-times-greater catalyst loading per square nanometer versus that of bulk alumina because more of the surface area is accessible to the catalyst for chemisorption as well as during catalytic turnover.

^{13}C CPMAS NMR spectroscopy employing ^{13}C-enriched organozirconium compounds indicates that electrophilic, "cation-like" organozirconium species are formed by two chemisorption pathways on the highly Brønsted acidic nanosized sulfated alumina. Chemisorption occurs primarily via a protonolytic M−CH$_3$ scission pathway at Brønsted acidic sites, whereas a small percentage reacts instead via methide transfer to the Lewis acidic sites. In either case, similar cationic organozirconium centers are formed, consistent with previous results on bulk AlS,[47] and are active catalysts for both olefin polymerization and arene hydrogenation. We also present here arene hydrogenation and olefin polymerization data for these organozirconium complexes supported on n-AlS. We conclude that nano-AlS provides a high-surface-area support-based activator for organozirconium complexes, forming cationic zirconium centers active for facile arene hydrogenations and production of high-molecular-weight polyethylene.

AUTHOR INFORMATION

Corresponding Author

*E-mail: t-marks@northwestern.edu.

ACKNOWLEDGMENT

We are grateful to the DOE for the support of this research under Grant 86ER1311, and to Ms. S. L. Wegener for her assistance with ICP measurements and helpful discussions. This work made use of the J. B. Cohen X-ray Diffraction Facility supported by the MRSEC program of the NSF (DMR-0520513) at the Materials Research Center of Northwestern University.

REFERENCES

(1) Dal Santo, V.; Liguori, F.; Pirovano, C.; Guidotti, M. *Molecules* **2010**, *15*, 3829–3856.
(2) Severn, J. R.; Chadwick, J. C.; Duchateau, R.; Friederichs, N. *Chem. Rev.* **2005**, *105*, 4073–4147.
(3) Thomas, J. M.; Raja, R.; Lewis, D. W. *Angew. Chem., Int. Ed.* **2005**, *44*, 6456–6482.
(4) Hlatky, G. C. *Chem. Rev.* **2000**, *100*, 1347–1376.
(5) Ribeiro, M. R.; Deffieux, A.; Portela, M. F. *Ind. Eng. Chem. Res.* **1997**, *36*, 1224–1237.
(6) Basset, J.-M.; Lefebvre, F.; Santini, C. *Coord. Chem. Rev.* **1998**, *178*, 1703–1723.
(7) Schatz, A.; Reiser, O.; Stark, W. J. *Chem.—Eur. J.* **2010**, *16*, 8950–8967.
(8) Li, K.-T.; Dai, C.-L.; Kuo, C.-W. *Catal. Commun.* **2007**, *8*, 1209–1213.
(9) Astruc, D.; Lu, F.; Aranzaes, J. R. *Angew. Chem., Int. Ed.* **2005**, *44*, 7852–7872.
(10) Thomas, J. M.; Raja, R. *Top. Catal.* **2006**, *40*, 3–17.
(11) Kantam, M. L.; Ghosh, S.; Aziz, K.; Sreedhar, B.; Choudary, B. M. *J. Mol. Catal., A* **2005**, *240*, 103–108.
(12) Amgoune, A.; Krumova, M.; Mecking, S. *Macromolecules* **2008**, *41*, 8388–8396.
(13) For examples in which reducing particle size to nanoscopic dimensions modifies catalytic properties, see: Moreno-Mañas, M.; Pleixats, R. *Acc. Chem. Res.* **2003**, *36*, 638–643.
(14) Haruta, M. J. *Nanoparticle Res.* **2003**, *5*, 3–4.
(15) Bell, A. T. *Science* **2003**, *299*, 1688–1691.
(16) Johnson, B. F.G. *Top. Catal.* **2003**, *24*, 147.
(17) Nicholas, C. P.; Marks, T. J. *Langmuir* **2004**, *20*, 9456–9462.
(18) Ahn, H.; Marks, T. J. *J. Am. Chem. Soc.* **2002**, *124*, 7103–7110.
(19) Li, Z.; Fredin, L. A.; Tewari, P.; DiBenedetto, S. A.; Lanagan, M. T.; Ratner, M. A.; Marks, T. J. *Chem. Mater.* **2010**, *22*, 5154–5164.
(20) Yigit, Z.; Inan, H. *Water, Air, Soil Pollut: Focus* **2009**, *9*, 237–243.
(21) Blanchard, J.; Abatzoglou, N.; Eslahpazir-Esfandabadi, R.; Gitzhofer, F. *Ind. Eng. Chem. Res.* **2010**, *49*, 6948–6955.
(22) Geng, Q.; Guo, Q.; Cao, C.; Wang, L. *Ind. Eng. Chem. Res.* **2008**, *47*, 2561–2568.
(23) Wang, T.; Wang, J.; Jin, Y. *Ind. Eng. Chem. Res.* **2007**, *46*, 5824–5847.

(24) Coates, G. W. *Chem. Rev.* **2000**, *100*, 1223–1252.
(25) Bhaduri, S., Mukesh, D., Eds.; *Homogenous Catalysis: Mechanisms and Industrial Applications*; John Wiley & Sons: New York, 2000; Vol. 1; pp 105−126.
(26) Amin, S. B.; Marks, T. J. *Angew. Chem., Int. Ed.* **2008**, *47*, 2006–2025.
(27) Kim, S. H.; Somorja, G. A. *Proc. Nat. Acad. Sci. U.S.A.* **2006**, *103*, 15289–15294.
(28) Kaminsky, W. J. *Polym. Sci., Part A: Polym. Chem.* **2004**, *42*, 3911–3921.
(29) Marks, T. J., Stevens, J. C., Eds.; *Top. Catal.* **1999**, *7*, 1 (special volume on "Advances in Polymerization Catalysis. Catalysts and Processes").
(30) Kaminsky, W. *Metalorganic Catalysts for Synthesis and Polymerization: Recent Results by Ziegler-Natta and Metallocene Investigations*; Springer-Verlag: Berlin, 1999.
(31) Britovsek, G. J. P.; Gibson, V. C.; Wass, D. F. *Angew. Chem., Int. Ed.* **1999**, *38*, 428–447.
(32) Jordan, R. F. *J. Mol. Catal.* **1998**, *128*, (special issue on "Metallocene and Single Site Olefin Catalysis") and references therein.
(33) Kaminsky, W.; Arndt, M. *Adv. Polym. Sci.* **1997**, *127*, 144–187.
(34) Brintzinger, H. H.; Fischer, D.; Mülhaupt, R.; Rieger, B.; Waymouth, R. M. *Angew. Chem., Int. Ed. Engl.* **1995**, *34*, 1143–1170.
(35) Soga, K., Terano, M., Eds.; *Catalyst Design for Tailor-Made Polyolefins*; Elsevier: Tokyo, 1994.
(36) Candy, J. P.; Coperet, C.; Basset, J.-M. *Top. Organomet. Chem.* **2005**, *16*, 151–210.
(37) Coperet, C.; Chabanas, M.; Saint-Arroman, R. P.; Basset, J.-M. *Angew. Chem., Int. Ed.* **2003**, *42*, 156–181.
(38) Sheldon, R. A., van Bekkum, H., Eds.; *Fine Chemicals through Heterogeneous Catalysis*; Wiley-VCH: Weinheim, 2001.
(39) Lindner, E.; Auer, F.; Baumann, A.; Wegner, P.; Mayer, H. A.; Bertagnolli, H.; Reinohl, U.; Ertel, T. S.; Weber, A. *J. Mol. Catal. A: Chem.* **2000**, *157*, 97–109.
(40) Lefebvre, F.; Basset, J.-M. *J. Mol. Catal. A: Chem* **1999**, *146*, 3–12.
(41) Scott, S. L.; Basset, J.-M.; Niccolai, G. P.; Santini, C. C.; Candy, J. P.; Lecuyer, C.; Quignard, F.; Choplin, A. *New J. Chem.* **1994**, *18*, 115–122.
(42) Iwasawa, Y.; Gates, B. C. *CHEMTECH* **1989**, *3*, 173–181, and references therein.
(43) Basset, J.-M., et al. , Eds.; *Surface Organometallic Chemistry: Molecular Approaches to Surface Catalysis*; Kluwer: Dordrecht, 1988.
(44) Iwasawa, Y. *Adv. Catal.* **1987**, *35*, 187–264.
(45) Williams, L. A.; Marks, T. J. *Organometallics* **2009**, *28*, 2053–2061.
(46) Motta, A.; Fragalá, I. L.; Marks, T. J. *J. Am. Chem. Soc.* **2008**, *130*, 16533–16546.
(47) Nicholas, C. P.; Ahn, H.; Marks, T. J. *J. Am. Chem. Soc.* **2003**, *125*, 4325–4331.
(48) Ahn, H.; Nicholas, C. P.; Marks, T. J. *Organometallics* **2002**, *21*, 1788–1806.
(49) Toscano, P. J.; Marks, T. J. *Langmuir* **1986**, *2*, 820–823.
(50) Eisen, M. S.; Marks, T. J. *J. Mol. Catal.* **1994**, *86*, 23–50.
(51) Marks, T. J. *Acc. Chem. Res.* **1992**, *25*, 57–65.
(52) Eisen, M. S.; Marks, T. J. *J. Am. Chem. Soc.* **1992**, *114*, 10358–10368.
(53) Finch, W. C.; Gillespie, R. D.; Hedden, D.; Marks, T. J. *J. Am. Chem. Soc.* **1990**, *112*, 6221–6232.
(54) Gillespie, R. D.; Burwell, R. L., Jr.; Marks, T. J. *Langmuir* **1990**, *6*, 1465–1477.
(55) Dahmen, K. H.; Hedden, D.; Burwell, R. L., Jr.; Marks, T. J. *Langmuir* **1988**, *4*, 1212–1214.
(56) Toscano, P. J.; Marks, T. J. *J. Am. Chem. Soc.* **1985**, *107*, 653–659.
(57) He, M.-Y.; Xiong, G.; Toscano, P. J.; Burwell, R. L., Jr.; Marks, T. J. *J. Am. Chem. Soc.* **1985**, *107*, 641–652.
(58) Conroy, K. D.; Hayes, P. G.; Piers, W. E.; Parvez, M. *Organometallics* **2007**, *26*, 4464–4470.
(59) Piers, W. E. *Adv. Organomet. Chem.* **2005**, *52*, 1–77.
(60) Stahl, N. G.; Salata, M. R.; Marks, T. J. *J. Am. Chem. Soc.* **2005**, *127*, 10898–10909.
(61) Metz, M. V.; Sun, Y.; Stern, C. L.; Marks, T. J. *Organometallics* **2002**, *21*, 3691–3702.
(62) Chen, Y.-X.; Kruper, W. J.; Roof, G.; Wilson, D. R. *J. Am. Chem. Soc.* **2001**, *123*, 745–746.
(63) Chen, E. Y.-X.; Marks, T. J. *Chem. Rev.* **2000**, *100*, 1391–1434 and references therein.
(64) Kristen, M. O. *Top. Catal.* **1999**, *7*, 89–95.
(65) Yang, X.; Stern, C. L.; Marks, T. J. *J. Am. Chem. Soc.* **1991**, *113*, 3623–3625.
(66) Kaminsky, W.; Kulper, K.; Brintzinger, H. H. *Angew. Chem., Int. Ed. Engl.* **1985**, *24*, 507–509.
(67) Benetollo, F.; Cavinato, G.; Crosara, L.; Milani, F.; Rossetto, G.; Scelza, C.; Zarella, P. *J. Organomet. Chem.* **1998**, *55*, 177–185.
(68) Wu, Y.; Liao, S. *Chem. Eng. China* **2009**, *3*, 330–343.
(69) Rode, C. V.; Garade, A. C.; Chikate, R. C. *Catal. Surv. Asia* **2009**, *13*, 205–220.
(70) Dasgupta, S.; Török, B. *Curr. Org. Synth.* **2008**, *5*, 321–342.
(71) Rao, L. *Resonance* **2007**, *12*, 65–75.
(72) Song, X.; Sayari, A. *Catal, Rev.−Sci. Eng.* **1996**, *38*, 329–412.
(73) Corma, A. *Chem. Rev.* **1995**, *95*, 559–614.
(74) Yamaguchih, T. *Appl. Catal.* **1990**, *61*, 1–25.
(75) Matsuhashi, H.; Motoi, H.; Arata, K. *Catal. Lett.* **1994**, *26*, 325–328.
(76) Arata, K. *Adv. Catal.* **1990**, *37*, 165–211.
(77) Lin, Z.; Marechal, J.-F. L.; Sabat, M.; Marks, T. J. *J. Am. Chem. Soc.* **1987**, *109*, 4127–4129.
(78) Williams, L. A.; Guo, N.; Motta, A.; Fragala, I. L.; Marshall, C. L.; Miller, J. T.; Marks, T. J. Manuscript in preparation.
(79) Arata, K. *Green Chem.* **2009**, *11*, 1719–1728.
(80) Matsuhashi, H.; Sato, D.; Arata, K. *React. Kinet. Catal. Lett.* **2004**, *81*, 183–188.
(81) Mekhemer, G. A. H.; Khalaf, H. A.; Mansour, S. A. A.; Nohman, A. K. H. *Monatshefte Chem.* **2005**, *136*, 2007–2016.
(82) Guzmàn-Castillo, M. L.; Lòpez-Salinas, E.; Fripiat, J. J.; Sànchez-Valente, J.; Hernàndez-Beltràn, F.; Dodrguez-Hernandez, A.; Navarrete-Bolaños, J. *J. Catal.* **2003**, *220*, 317–325.
(83) Escalona, P. E.; Penarroya, M. M.; Morterra, C. *Langmuir* **1999**, *15*, 5079–5087.
(84) Yang, T.; Chang, T.; Yeh, C. *J. Mol. Catal. A: Chem.* **1997**, *123*, 163–169.
(85) Yang, T.; Chang, T.; Yeh, C. *J. Mol. Catal. A: Chem.* **1997**, *115*, 339–346.
(86) Arata, K.; Hino, M. *Appl. Catal.* **1990**, *59*, 197–204.
(87) Przystajko, W.; Fiedorow, R.; Dalla Lana, I. G. *Appl. Catal.* **1985**, *15*, 265–275.
(88) Hino, M.; Arata, K. *Chem. Lett.* **1979**, 477–480.
(89) Arata, K.; Hino, M. *React. Kinet. Catal. Lett.* **1984**, *25*, 143–145.
(90) Matsuhashi, H.; Hino, M.; Arata, K. *Catal. Lett.* **1991**, *8*, 269–272.
(91) Chavan, S.; Zubaidha, P. K.; Dantale, S. W.; Keshavaraja, A.; Ramaswamy, A. V.; Ravindranathan, T. *Tetrahedron Lett.* **1996**, *37*, 233–236.
(92) Matsuhashi, H.; Hino, M.; Arata, K. *Appl. Catal.* **1990**, *59*, 205–212.
(93) Matsuhashi, H.; Hino, M.; Arata, K. *Chem. Lett.* **1988**, 1027–1028.
(94) Chen, J. P.; Yang, R. T. *J. Catal.* **1993**, *139*, 277–288.
(95) Hino, M.; Arata, K. *J. Chem. Soc., Chem. Commun.* **1979**, 1148–1149.
(96) Reddy, B. M.; Patil, M. K. *Chem. Rev.* **2009**, *109*, 2185–2208.
(97) Nicholas, C. P.; Marks, T. J. *Nano Lett.* **2004**, *4*, 1557–1559.
(98) Valente, J. S.; Lopez-Salinas, E.; Bokhimi, X.; Flores, J.; Maubert, A. M.; Lima, E. *J. Phys. Chem. C.* **2009**, *113*, 16476–16484.
(99) Wolczanski, P. T.; Bercaw, J. E. *Organometallics* **1982**, *1*, 793–799.

(100) Manriquez, J. M.; McAlister, D. R.; Sanner, R. D.; Bercaw, J. E. *J. Am. Chem. Soc.* **1978**, *100*, 2716–2724.
(101) Oppolzer, W.; Mirza, S. *Helv. Chim. Acta* **1984**, *67*, 730–738.
(102) Escalona, P. E.; Penarroya, M. M.; Morterra, C. *Langmuir* **1999**, *15*, 5079–5087.
(103) Yang, T.; Chang, T.; Yeh, C. *J. Mol. Catal. A: Chem.* **1997**, *123*, 163–169.
(104) NMR scale activation of $Cp^*_2Zr(^{13}CH_3)_2$ with $B(C_6F_5)_3$ in C_6D_6.
(105) Jezequel, M.; Dufaud, V.; Ruiz-Garcia, M. J.; Carrillo-Hermosilla, F.; Neugwbauer, U.; Niccolai, G. P.; Lefebvre, F.; Bayard, F.; Corker, J.; Fiddy, S.; Evans, J.; Broyer, J.-P.; Malinge, J.; Basset, J.-M. *J. Am. Chem. Soc.* **2001**, *123*, 3520–3540.
(106) Chen, H. Y.; Chum, S. P.; Hiltner, A.; Baer, E. *J. Polym. Sci., Part B: Polym. Phys.* **2001**, *37*, 1578–1593.